G-centers in irradiated silicon revisited: A screened hybrid density functional theory approach

Wang, H. , Chroneos, A. , Londos, C.A. , Sgourou, E.N. and Schwingenschlögl, U

Original citation:
Wang, H. , Chroneos, A. , Londos, C.A. , Sgourou, E.N. and Schwingenschlögl, U. (2014) G-centers in irradiated silicon revisited: A screened hybrid density functional theory approach. Journal of Applied Physics, volume 115 (Article number 183509). DOI: 10.1063/1.4875658

http://dx.doi.org/10.1063/1.4875658

American Institute of Physics

G-centers in irradiated silicon revisited: a screened hybrid density functional theory approach

H. Wang,[1] A. Chroneos,[2,3,a)] C. A. Londos,[4] E. N. Sgourou,[4] and U. Schwingenschlögl[1,b)]

[1]*PSE Division, KAUST, Thuwal 23955-6900, Saudi Arabia*
[2]*Engineering and Innovation, The Open University, Milton Keynes MK7 6AA, United Kingdom*
[3]*Department of Materials, Imperial College, London SW7 2AZ, United Kingdom*
[4]*University of Athens, Solid State Physics Section, Panepistimiopolis Zografos, Athens 157 84, Greece*

PACS: 71.15.Mb ; 71.55.Cn

Electronic structure calculations employing screened hybrid density functional theory are used to gain fundamental insight into the interaction of carbon interstitial (C_i) and substitutional (C_s) atoms forming the C_iC_s defect known as G-center in silicon (Si). The G-center is one of the most important radiation related defects in Czochralski grown Si. We systematically investigate the density of states and formation energy for different types of C_iC_s defects with respect to the Fermi energy for all possible charge states. Prevalence of the neutral state for the C-type defect is established.

[a)]Alex.Chroneos@open.ac.uk ; [b)]Udo.Schwingenschlogl@kaust.edu.sa

I Introduction

Silicon (Si) is an important material for numerous devices (e.g. microelectronic and photovoltaic) though its electronic properties and defect processes are significantly affected by the presence of impurities,[1-6] where carbon (C) is a common impurity in the mono-crystalline Si lattice and is incorporated inadvertently during the Czochralski growth process.[7,8] C is isovalent with Si and occupies electrically neutral substitutional sites (C_s). Its presence is evidenced in the IR spectra by a localized vibrational mode (LVM) at 607 cm^{-1}. It is established[9,10] that most of the Si self-interstitials (Si_I) are readily trapped by C_s defect, which are shifted off lattice sites so that C interstitials (C_i) form. Importantly, radiation defects such as C_iC_s pairs introduce[11,12] electronic levels in the Si band gap, affecting the efficiency of corresponding devices. In general, the performance of Si as optical emitter is limited by its indirect band gap, where introduction of optically active C-related G-centers is a promising approach to improve the efficiency because the sharp luminescence peak at 1.28 μm matches the important optical communications wavelength of 1.30 μm. It has been demonstrated that G-centers can contribute to optically pumped lasing.[13,14] The emission of G-center results from the existence of bistable configurations of the C_iC_s defect, the formation of which is assisted by mobile Si_I defect. Various approaches have been put forward to introduce G-centers, such as high concentration C doping[14], nano-patterning of the Si surface[7], and C implantation followed by proton irradiation.[15] Song *et al.*[16] has reported two configurations of the C_iC_s defect according to their structural, electronic, and optical properties obtained by a variety of experiments. Interestingly, a third configuration of the C_iC_s defect has been identified theoretically not long ago,[17,18] using the local density

approximation or generalized gradient approximation. However, both these approximations underestimate the band gap of pristine Si so that a more sophisticated approach has to be employed[19]. For this reason, we use in our work screened hybrid density functional theory calculations to investigate the densities of states (DOSs) and formation energies of the three known types of the C_iC_s defect with respect to the Fermi energy for all possible charge states.

II Methodology

The Vienna Ab-initio Simulation Package[20] is used with pseudopotentials generated by the projector augmented wave method[21] and a 2×2×2 supercell containing 64 Si atoms. The k-point mesh is set to 3×3×3 within the Monkhorst-Pack scheme[22] and the cutoff energy for the plane waves amounts to 400 eV. The lattice constant of Si is optimized employing the PBEsol[23] functional, which gives results very close to those obtained by screened hybrid functional Heyd, Scuseria, and Ernzerhof (HSE) calculations.[24-26] A Gaussian smearing with a width of 0.05 eV is used. For each charged defect, the lattice constant is kept at the value of pristine Si and the atomic positions are relaxed until the forces on all atoms decline below 0.01 eV/Å. The optimized structures are then used for HSE calculations with Perdew, Burke, and Ernzerhof local term and a screening parameter of $\mu = 0.206$ Å^{-1}. Finally, we apply the correction approach of by Freysoldt *el al.*[27,28] to our finite size supercell calculations to eliminate artificial interaction.

The formation energy of the C_iC_s defect with respect to the Fermi energy for all possible charge states is given by[29]

$$\Delta H_{D,q}(\mu_e\, \mu_a) = E_{D,q} - E_H + \sum n_a\, \mu_a + q\, \mu_e$$

where $E_{D,q}$ is the total energy of the defective cell with charge q and E_H is the total energy of the perfect cell. Moreover, n_a represents the number of atoms added or removed to the defective cell and μ_a corresponds to their chemical potentials. The Fermi energy is denoted as μ_e and is measured from the top of the valence band maximum, with values in the band gap: $E_{\mathrm{VBM}} \leq \mu_e \leq E_{\mathrm{VBM}} + E_{gap}$. The C chemical potential is calculated using face-centered cubic SiC.

III Results and discussion

The efficacy of the present computational approach has been discussed in a recent study on vacancies and the A-center in Si,[30,31] which we here extend to the case of the G-center. Two stable structural configurations of C_iC_s (A- and B-type[16]) are shown in Figs. 1(a) and (b), whereas the more recently predicted C-type configuration[17,18] is depicted in Fig. 1(c). The established A- and B-type configurations will be discussed first. In the A-type structure the substitutional C atom, bonding with four Si atoms, is denoted as C(4). The C interstitial sharing a regular lattice site with a Si atom is denoted as C(3) and the Si atom connecting two C atoms as Si(2C). The four C(4)-Si bond distances are 1.88 Å, 1.99 Å, 1.99 Å, and 2.03 Å and the three C(3)-Si bond distances amount to 1.75 Å, 1.83 Å, and 1.83 Å, while the Si-Si bond length is 2.36 Å. As compared with the A-type defect, the Si(2C)-Si bond breaks and one C-Si bond forms in the B-type case. The C interstitial now fully occupies the Si site. The two groups of C(4)-Si bond lengths become 1.85 Å, 1.94 Å, 2.01 Å, 2.01 Å, and 1.88 Å, 1.96 Å, 1.96 Å, 2.04 Å. In general, the geometrical properties obtained in the present study are in agreement with the results

reported previously.[32,33]

The partial DOSs for the two C atoms and Si(2C) in 0, +1, and -1 charged A- and B-type structures are depicted in Fig. 2. Other Si atoms have similar DOSs without significant peaks around the Fermi level and are thus not shown. As in A-type $C_iC_s^0$ the C(3) atom has one dangling electron, the DOS reveals a sharp peak below the Fermi level. In addition, the Si(2C) atom shows very localized unoccupied states around 6.5 eV, because of its two C nearest neighbors with a much larger electronegativity. This is also illustrated by the DOS of B-type $C_iC_s^0$. As a consequence, when an electron is trapped by the C_iC_s defect it will occupy the Si(2C) states, as shown in the DOSs of A- and B-type $C_iC_s^{-1}$. In the B-type configuration, since the C interstitial becomes fourfold coordinated, the Si(2C) atom receives more valence charge, which results in the peak below the Fermi level. Because both C atoms have fourfold coordinations, there appears no distinct C peak in the DOS.

The experimental total energy differences indicate that the A-type defect is more stable than the B-type defect for +1 and -1 charge, whereas the B-type defect is more stable for 0 charge. Table I summarized the experimental results[16] and the calculated total energy differences between the A- and B-type structures. The results obtained by the PBEsol functional only agree with the experimental value in the energetic order for the charge neutral state, while the value is substantially larger. Our HSE calculations yield results that agree with the experiment better than previous theoretical studies[32-34], except for the -1 charge state for which the total energy difference is 0.07 eV while the experimental value is -0.04 eV. The total energy difference for the charge neutral state is found to be 0.04 eV, which is very close to the experimental value of 0.02 eV, and for the

+1 charge state the value of -0.09 eV is also qualitatively comparable to the experimental result of -0.02 eV. Spin polarized calculations are performed using both the PBEsol and HSE functionals. For the HSE functional, only the total energies of A-type $C_iC_s^{+1}$ and B-type $C_iC_s^{+1}$ and $C_iC_s^{-1}$ are lowered in energy (as compared to the spin-degenerate solution) by significant amounts of 0.22 eV, 0.02 eV, and 0.07 eV, respectively. Therefore, the energy difference between the A- and B-type defects becomes -0.29 eV for the +1 charge state and 0.14 eV for the -1 charge state. We have also performed calculations for 128-atom supercell on the PBEsol level and show the results in Table I, confirming the PBEsol 64-atom results. This indicates that the 64-atom supercell is large enough to avoid artificial effects of the strain field.

The spin polarized partial DOSs for the A- and B-type $C_iC_s^{+1}$ and $C_iC_s^{-1}$ defects are shown in Fig. 3. For A-type $C_iC_s^{+1}$ the occupied states of the C(3) atom delocalize in energy, the unoccupied states shift to higher energy, and a significant magnetic moment (within the atomic sphere) of 0.29 μ_B is obtained. The DOSs of the C atoms in A-type $C_iC_s^{-1}$ is almost spin degenerate with a magnetic moment of 0.17 μ_B localized on Si(2C). For B-type $C_iC_s^{+1}$ and $C_iC_s^{-1}$, respectively, the donated and accepted charge is mainly localized on Si(2C) with a magnetic moment of 0.16 μ_B and 0.13 μ_B. These results agree with the experimental situation[16] in two points: The electron paramagnetic resonance signal of C in A-type $C_iC_s^{-1}$ is much weaker than for $C_iC_s^{+1}$ and the unpaired spin is much less localized on C atoms in the B-type $C_iC_s^{-1}$ than in A-type $C_iC_s^{+1}$. Nevertheless, the experimental finding that the unpaired spin spreads over the neighboring Si atoms of the A- and B-type $C_iC_s^{-1}$ defects is not reproduced by the calculations (the magnetic moments on other atoms are one order of magnitude smaller than those on Si(2C)). This may be the

reason why the theoretical energy difference between A- and B-type $C_iC_s^{-1}$ is not consistent with the experimental value.

Figures 4(a) and 4(b) present the formation energy of the C_iC_s defect as function of the Fermi energy for different charge states. Note that the total energies of A-type $C_iC_s^{+1}$ and B-type $C_iC_s^{-1}$ from the spin polarized calculations are used. Except for the fact that the A-type defect has a higher (+/0) transition level, the results are similar due to the small total energy difference between the A- and B-type configurations in other charge states. In the low Fermi energy range the +1 charge state is favorable, while at higher Fermi energy the charge neutral state dominates. The transition levels between different charge states are reported in Table II for all configurations considered.

A third configuration of the C_iC_s defect has been revealed in Refs. 17, 18 to be more stable than the A- and B-types. In this C-type configuration, as shown in Fig. 2(c), the C-C atom pair along the <100> direction occupies a regular Si lattice site. The C-C bond length is 1.42 Å, which is shorter than that in diamond or graphite. The C-Si interaction is weaker than the C-C interaction as reflected by longer C-Si bonds (1.89 Å). In addition, the fact that each C atom has a dangling electron is demonstrated by the half-occupied peaks at the Fermi level in the spin degenerate DOS of charge neutral C-type C_iC_s in Fig. 5. An average DOS is shown because the results for the C atoms as well as for its nearest Si neighbors are similar. Spin polarization splits these peaks and results in magnetic moments on the C atoms. For the +1/-1 charge states the wave function of the lost/trapped electron is shared by both C atoms, as demonstrated by the fact that the DOS curve of each C atom in $C_iC_s^{+}$ and $C_iC_s^{-}$ crosses the Fermi level. The total energy of the charge neutral C-type defect is 0.11 eV higher than found for the A-type defect in the

spin degenerate calculation, but 0.61 eV lower in the spin polarized case, which is comparable to the value of 0.2 eV[17] as obtained by the generalized gradient approximation. In addition, spin polarization lowers the total energies of the +1 and -1 charge states by 0.20 eV and 0.23 eV, respectively. The formation energy for the different charge states of C-type C_iC_s as a function of the Fermi energy is plotted in Fig. 4(c), presenting results for the spin polarized 0, +1, and -1 charge states. The +2 and -2 charge states are favorable in small ranges at low and high Fermi energy, respectively, while the charge neutral state is favorable in the Fermi energy range from 0.06 eV to 0.91 eV due to that fact that the two unpaired electrons on the C atoms, under spin polarization, lower the total energy substantially. The transition between the other charge states occurs somewhere in the middle of the band gap.

IV Conclusions

In conclusion, screened hybrid density functional theory calculations have been used to investigate the electronic properties of G-centers in Si. The calculated formation energies show that neutral charge state is favorable in most of the Fermi energy range. For the A- and B-type metastable C_iC_s structures HSE functional calculations have been demonstrated to yield significantly improved agreement with the experimental situation with respect to the energetic order, as compared to previous theoretical work. The two unpaired electrons on the C atoms in C-type C_iC_s lead to spin polarization. Importantly, the C-type C_iC_s configuration is revealed to the lowest energy, calling for in-depth experimental research on the C-type G-center.

References

[1]L. I. Murin, E. A. Tolkachava, V. P. Markevich, A. R. Peaker, B. Hamilton, E. Monakhov, B. G. Svensson, J. L. Lindström, P. Santos, J. Coutinho, and A. Carvalho, Appl. Phys. Lett. **98**, 182101 (2011).

[2]G. Davies, Phys. Rep. **176**, 83 (1989).

[3]R. Laiho, M. P. Vlasenko, and L. S. Vlasenko, Solid State Comm. **124**, 403 (2002).

[4]A. Chroneos, C. A. Londos, E. N. Sgourou, and P. Pochet, Appl. Phys. Lett. **99**, 241901 (2011).

[5]M. Forster, E. Fourmond, F. E. Rougieux, A. Cuevas, R. Gotoh, K. Fujiwara, S. Uda, and M. Lemiti, Appl. Phys. Lett. **100**, 042110 (2012).

[6]P. Chen, X. Yu, X. Liu, X. Chen, Y. Wu, and D. Yang, Appl. Phys. Lett. **102**, 082107 (2013).

[7]R. C. Newman, Mat. Res. Soc. Symp. Proc. **59,** 403 (1986).

[8]W. Scorupa and R. A. Yankov, Mater. Chem. Phys. **44** , 101 (1996).

[9]R. C. Newman and A. R. Bean, Radiat. Eff. **8**, 189 (1970).

[10]G. D. Watkins and K. L. Brower, Phys. Rev. Lett. **36**, 1329 (1976).

[11]S. D. Brotherton and P. Bradley, J. Appl. Phys. **53**, 5720 (1982).

[12]K. Murata, Y. Yasutake, K. Nittoh, S. Fukatsu, and K. Miki, AIP Adv. **1**, 032125 (2011).

[13]S. G. Cloutier, P. A. Kossyrev, and J. Xu, Nat. Mater. **4**, 877 (2005).

[14]E. Rotem, J. M. Shainline, and J. M. Xu, Appl. Phys. Lett. **91**, 051127 (2007).

[15]D. D. Berhanuddin, M. A. Lourenço, R. M. Gwilliam, and K. P. Homewood, Adv. Funct. Mater. **22**, 2709 (2012).

[16]L. W. Song, X. D. Zhan, B. W. Benson, and G. D. Watkins, Phys. Rev. B **42**, 5765 (1990).

[17]C.-L. Liu, W. Windl, L. Borucki, S. Lu, and X.-Y. Liu, Appl. Phys. Lett. **80**, 52 (2002).

[18]F. Zirkelbach, B. Stritzker, K. Nordlund, J. K. N. Lindner, W. G. Schmidt, and E. Rauls, Phys. Rev. B **82**, 094110 (2010); Phys. Rev. B **84**, 064126 (2011).

[19]J. Heyd, J. E. Peralta, G. E. Scuseria, and R. L. Martin, J. Chem. Phys. **123**, 174101 (2005).

[20]G. Kresse and D. Joubert, Phys. Rev. B **59**, 1758 (1999).

[21]P. E. Blöchl, Phys. Rev. B **50**, 17953 (1994).

[22]H. J. Monkhorst and J. D. Pack, Phys. Rev. B **13**, 5188 (1972).

[23]J. P. Perdew, A. Ruzsinszky, G. I. Csonka, O. A. Vydrov, G. E. Scuseria, L. A. Constantin, X. Zhou, and K. Burke, Phys. Rev. Lett. **100**, 136406 (2008).

[24]J. Heyd, G. E. Scuseria, and M. Ernzerhof, J. Chem. Phys. **118**, 8207 (2003).

[25]L. Schimka, J. Harl, and G. Kresse, J. Chem. Phys. **134**, 024116 (2011).

[26]T. M. Henderson, J. Paier, and G. E. Scuseria, Phys. Status Solidi B **248**, 767 (2011).

[27]C. Freysoldt, J. Neugebauer, and C. G. van de Walle, Phys. Rev. Lett. **102**, 016402 (2009).

[28]C. Freysoldt, J. Neugebauer, and C. G. van de Walle, Phys. Stat. Sol. B **248**, 1067 (2011).

[29]S. Lany and A. Zunger, Phys. Rev. B **78**, 235104 (2008).

[30]H. Wang, A. Chroneos, C. A. Londos, E. N. Sgourou, and U. Schwingenschlögl, Appl. Phys. Lett. **103**, 052101 (2013).

[31]H. Wang, A. Chroneos, D. Hall, E. N. Sgourou, and U. Schwingenschlögl, J. Mater. Chem A **1**, 11384 (2013).

[32]P. Leery, R. Jones, S. Öberg, and V. J. B. Torres, Phys. Rev. B **55**, 2188 (1997).

[33]R. B. Capaz, A. Dal Pino Jr, and J. D. Joannopoulos, Phys. Rev. B **58**, 9845 (1998).

[34]M. J. Burnard and G. G. DeLeo, Phys. Rev. B **47**, 10217 (1993).

TABLE I Total energy differences (eV) between the ground states of the A- and B-type structures of the C_iC_s defect for different charges. The numbers in brackets are obtained by spin polarized calculations.

	$A^+ - B^+$	$A^0 - B^0$	$A^- - B^-$
Experiment [16]	-0.02	0.02	-0.04
PBEsol 64 atoms	0.15	0.20	0.23
HSE 64 atoms	-0.09(-0.29)	0.04	0.07(0.14)
PBEsol 128 atoms	0.14	0.18	0.21

TABLE II. Calculated transition levels (in eV) between different charge states for C_iC_s defects.

	A-type	B-type	C-type
(++/+)	---	---	0.16
(++/0)	0.16	0.12	0.06
(+/0)	0.39	0.25	---
(0/-)	---	---	1.05
(0/--)	---	---	0.91
(+/-)	0.73	0.74	0.50
(+/--)	0.93	1.03	0.59
(++/-)	0.46	0.49	0.39
(-/--)	---	---	0.76
(++/--)	0.68	0.77	0.48

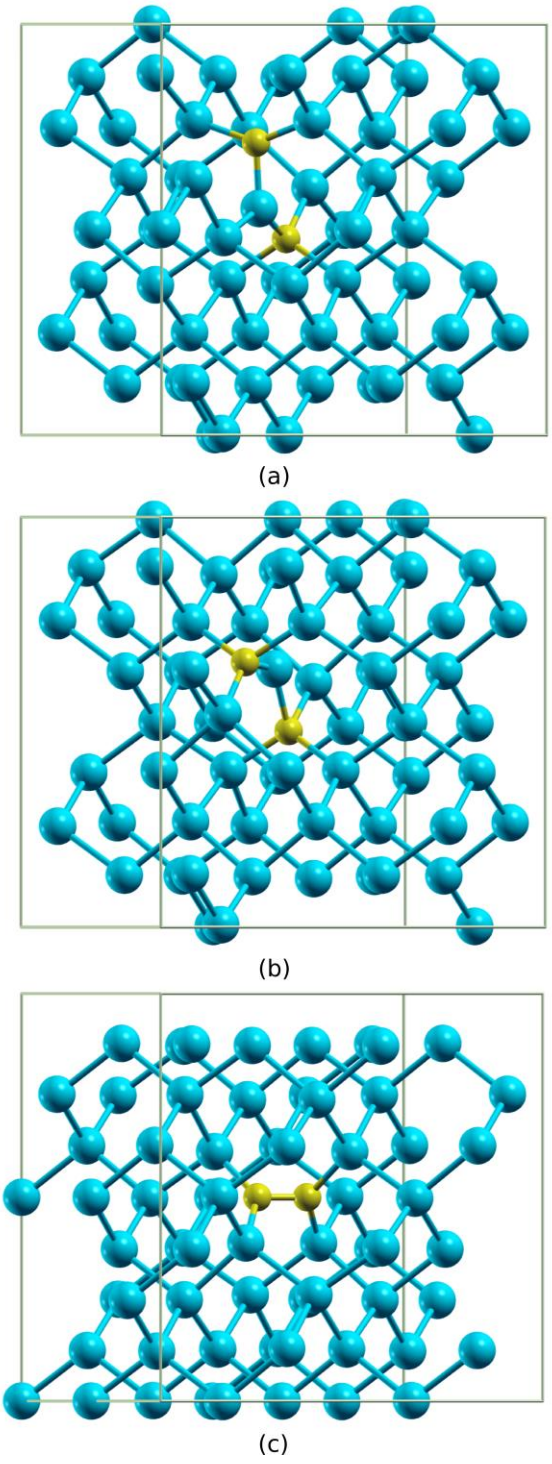

FIG. 1. (Color online) Structures of the A-type (a), B-type (b), and C-type (c) C_iC_s defects. Big blue spheres are Si atoms and medium yellow spheres are C atoms.

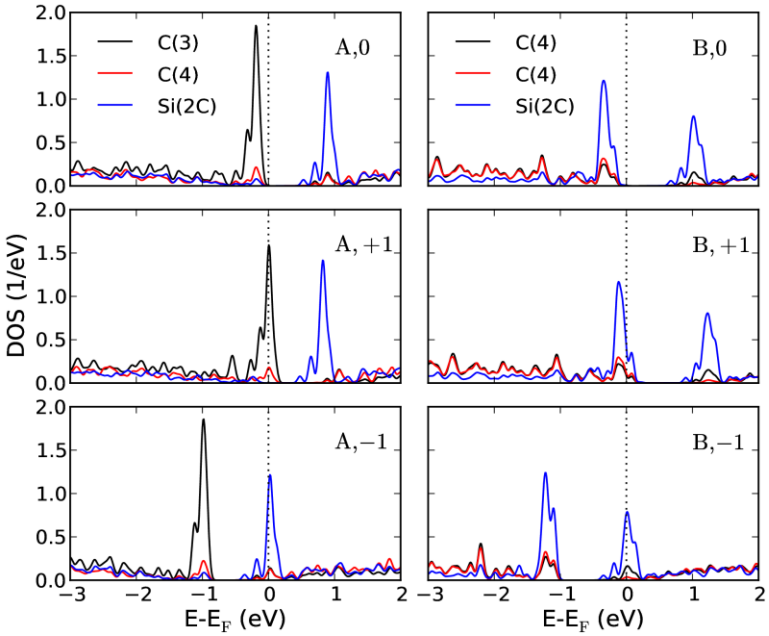

FIG. 2. (Color online) Spin degenerate partial DOSs of A- and B-type C_iC_s defects in 0, +1, and -1 charge states. C(3) and C(4) indicate the C atoms coordinated by three and four Si atoms, respectively. Si(2C) is the Si atom that connects two C atoms. The states below the dotted line are occupied.

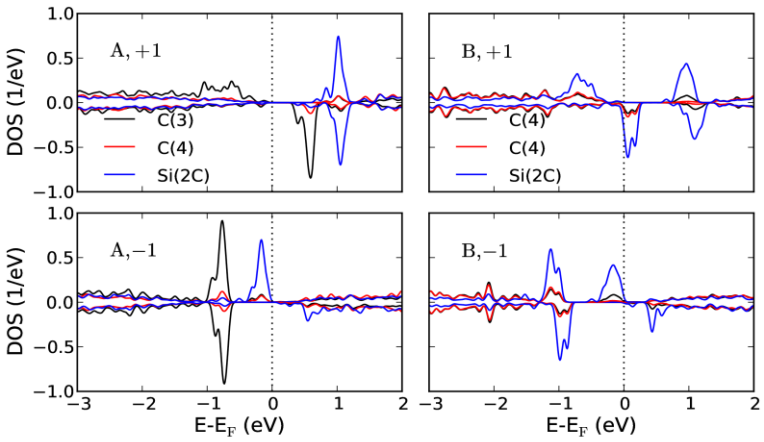

FIG. 3. (Color online) Spin polarized partial DOSs of the A- and B-type C_iC_s defects in the +1 and -1 charge states. C(3) and C(4) indicate the C atoms coordinated by three and four Si atoms, respectively. Si(2C) is the Si atom that connects two C atoms. The states below the dotted line are occupied.

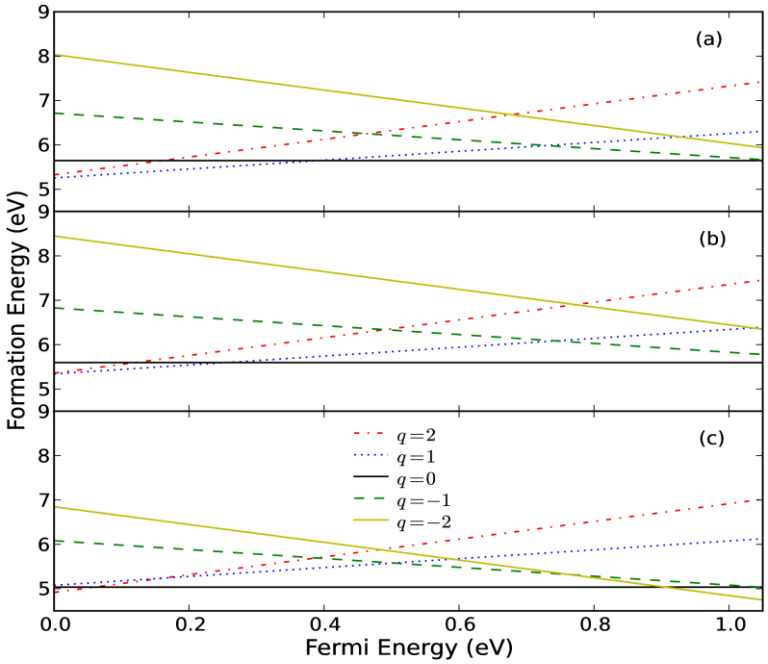

FIG. 4. (Color online) Formation energies of the A-type (a), B-type (b), and C-type (c) C_iC_s defects with respect to the Fermi energy.

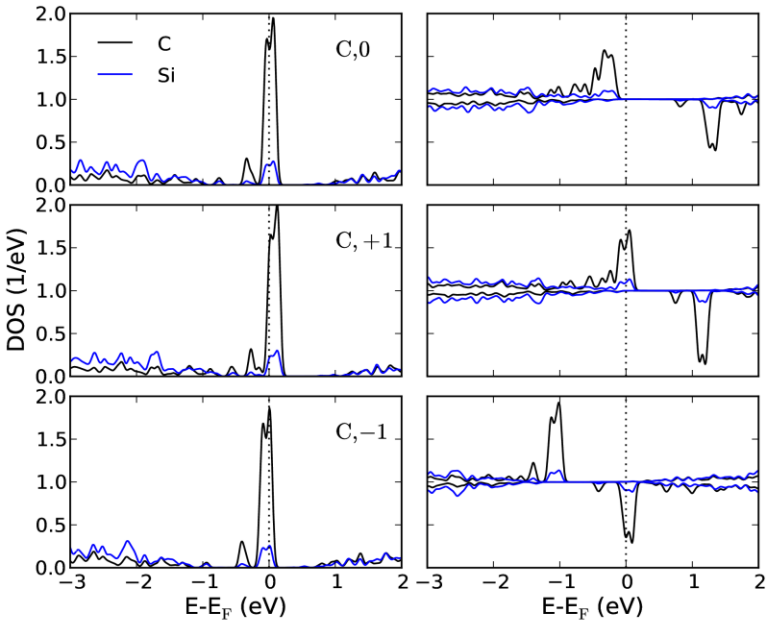

FIG. 5 (Color online) Spin degenerate and spin polarized partial DOSs of C-type C_iC_s in the 0, +1, and -1 charge states. The average DOS of the C atoms and of the nearest Si neighbors is shown. The states below the dotted line are occupied.